Solar Energy Materials & Solar Cells 209 (2020) 110456

Contents lists available at ScienceDirect

Solar Energy Materials and Solar Cells

journal homepage: http://www.elsevier.com/locate/solmat

Enhancing passive radiative cooling properties of flexible CIGS solar cells for space applications using single layer silicon oxycarbonitride films

Udayan Banik [a,*], Kaname Sasaki [b], Nies Reininghaus [a], Kai Gehrke [a], Martin Vehse [a], Maciej Sznajder [b], Tom Sproewitz [b], Carsten Agert [a]

[a] DLR Institute of Networked Energy Systems, 26129, Oldenburg, Germany
[b] DLR Institute of Space Systems, 28359, Bremen, Germany

ARTICLE INFO

Keywords:
Polysilazane coating
Flexible CIGS solar cells
Mid-infrared emittance
Satellite solar array
Thermo-electrical properties
Durazane 1800

ABSTRACT

Satellites in lower earth orbits have been primarily powered by photovoltaic modules. With growing power demand for new satellite concepts, solar cells are required to be flexible and ultra-lightweight to decrease launch costs. CIGS thin film solar technology is a promising candidate, since it can be manufactured on flexible substrates and possesses high radiation hardness. Poor radiative properties of CIGS on the other hand, lead to high temperatures and therefore power loss. High emissivity coatings on CIGS have already been reported but the influence on thermal and electrical aspects have not been addressed. Here we present the optical properties of silicon-oxycarbonitride coatings and their effect on electrical parameters on CIGS cells to be used for the DLR's GoSolAr power sail mission. We show that the single layer coating can significantly increase emissivity from 0.3 to 0.72, with minimal spectral losses and negligible impact on the functioning of the underlying CIGS cell. We simulated the thermal impact of the coating on solar cells in orbit and can predict that the maximum temperature of the cells is reduced by 30 °C, resulting in a significant power gain. Additionally, the coating has an emissivity of 0.87 in the atmospheric window of 8–13 μm making it a very good passive radiative cooler for terrestrial solar cells. The low-cost coating can replace glass and the process can be scaled up for large CIGS modules. The coating can also significantly increase the power to mass ratio of solar modules, reducing costs for space applications.

1. Introduction

Cover glasses on solar cells provide shielding from high energy particles in space. Additionally, the solar cells benefit from the high emissivity of glass which allows better emittance of heat into space. However, the low specific mass and flexibility advantage of thin film technology is lost when a conventional rigid panel array design with several millimeter of thick glass is used [1]. Among thin film PV, CIGS solar cells on flexible lightweight substrates such as polyimide or stainless steel have attracted particular attention for use in outer space and high-altitude platforms. They have superior tolerance to radiation, high power to mass ratio, high power to stowed volume ratio and low cost of production [2]. CIGS cell technology has been investigated for radiation hardness in the past. Electrical performance data of CIGS cells on MDS-1 and SOHLA-1 satellites by JAXA confirmed negligible degradation due to radiation in orbit [3–5]. Lab based studies have shown self-annealing effects in CIGS from defects caused by high energy particles at around 100 °C. Thermal annealing of the irradiated solar cells was found to restore initial short circuit current by annihilating deep defect states [6]. It was also observed that the activation energy required for annealing rates from proton damages, decreases for cells exposed to AM0 light than cells kept in dark [7]. These recovery conditions are easily achievable in LEO and such high radiation hardness would even allow the use of CIGS cells without cover glass. A major challenge in using this solar technology for space applications is that CIGS cells have a very low emissivity (0.18–0.3) in the IR region due to its high reflection in the IR spectral range [2,8]. A bare CIGS cell in space will encounter high temperatures (above 100 °C) in orbit which will result in power loss due to its low emissivity and inherent negative temperature coefficient [9]. Therefore, there is a requirement for a coating, which combines high transparency in UV–Vis region for the efficient operation of the solar cell and high broad band emissivity in the MIR to facilitate radiative cooling.

The GoSolAr mission by DLR aims to demonstrate the reliability of thin film PV technologies in powering spacecraft with applications that

* Corresponding author.
E-mail addresses: udayan.banik@dlr.de (U. Banik), kaname.sasaki@dlr.de (K. Sasaki), nies.reininghaus@dlr.de (N. Reininghaus), kai.gehrke@dlr.de (K. Gehrke), martin.vehse@dlr.de (M. Vehse), maciej.sznajder@dlr.de (M. Sznajder), tom.sproewitz@dlr.de (T. Sproewitz), carsten.agert@dlr.de (C. Agert).

https://doi.org/10.1016/j.solmat.2020.110456
Received 8 October 2019; Received in revised form 8 January 2020; Accepted 7 February 2020
Available online 18 February 2020

Abbreviations

DLR	German Aerospace Center
CIGS	Copper indium gallium di-selenide
GoSolAr	Gossamer Solar Array
LEO	Lower Earth orbit
MIR	Mid infrared
IR	Infrared
JAXA	Japan Aerospace Exploration Agency
UV–Vis	Ultraviolet–Visual
PV	Photovoltaic
PSZ	Polysilazane
PDC	Polymer derived coating
CFRP	Carbon fiber reinforced plastic
FTIR	Fourier transform infrared spectroscopy
SEM	Scanning electron microscope
FIB	Focused ion beam
ECSS	European cooperation for space standardization
IV	Current-voltage
EQE	External quantum efficiency
AM	Air mass
SiCNO	Silicon oxycarbonitride

require high power such as electric propulsions, space tugs etc. [10,11]. It plans to demonstrate deployability and operational functioning of a 5 m × 5 m flexible PV blanket in LEO. Continuous IV sweeps of the modules during the mission lifetime, particle irradiation and atomic oxygen along with solar irradiation will be monitored and telemetered. Every 17 cm × 17 cm PV module will be equipped with a thin film temperature sensor in a sandwich configuration on the carrier membrane which will be monitored as well. The PV blanket will be launched in a stowed configuration of 60 cm × 60 cm x 48 cm. It will be structurally supported and deployed using rollable 2D CFRP booms [12]. For an ultra-lightweight module design, as in GoSolAr, cooling of PV by passive radiative process was identified as practical and feasible. The application process of the coating should be simple, processed at low temperatures, and scalable to large areas. The whole process and the coating should not degrade or be detrimental to the functioning of the solar cells.

Emissivity enhancing coatings for CIGS have been under investigation for some time. Shimazaki et al. [8]. investigated a double coating system using electron beam deposition to achieve $\varepsilon = 0.78$. Pscherer et al. [13] and Günthner et al. [14] have previously investigated flexible PDCs on CIGS with polyimide substrates achieving $\varepsilon = 0.77$. Atomic oxygen protective properties and effects of vacuum ultraviolet radiation of PDCs have also been studied [15,16]. Optical meta-surfaces with multilayer structure and microstructures have also been proposed and investigated recently to enhance radiative emission properties with coatings [17–19]. However, the thermal impact and consequences on electrical performance of CIGS cells due to the PDCs have not been investigated.

In this paper we demonstrate the properties of a single layer polymer derived coating of SiCNO deposited by dip coating. Commercially available organopolysilazane was used as a precursor in conjunction to CIGS cells on polyimide substrates. Optical properties of the coating and electrical impact of the coating on solar cells were investigated in detail. The change in emissivity has been measured as a function of coating thickness and hoisting speed. We report the highest emissivity of 0.72 achieved with a single layer coating (~3.2 μm) using Durazane 1800 as precursor. The findings of this investigation complement those of the earlier studies with double layers or engineered polysilazane precursor materials [13,14]. These findings extend our understanding of such coating and establish its positive impact on the thermal management and electrical performance of the solar cells with regards to space applications. We did not address the flexibility of the coating itself due to design considerations, as the folding occurs in the membrane material but not on the PV modules. Nevertheless, the coating shows good adherence and enough flexibility for handling purposes. We evaluated the thermal impact of the coating on solar cells for the proposed orbit of the GoSolAr mission. Analysis based on experimental and simulation results show that a ~3 μm coating can enhance the emissive power of the CIGS solar cell by 123% resulting in an extra ~260 Wh of energy production per orbit for the GoSolAr payload.

2. Radiative cooling

Every physical body at non-zero Kelvin temperature shows thermal emission in the form of electromagnetic radiation. For a theoretical black body ($\varepsilon = 1$ for all wavelengths) the spectral radiation intensity is a function of the temperature of the body as described by Planck's law. Both the temperature and spectral emissivity of the body determine the radiative potential since total emissivity of a real body is never unity or constant (like gray bodies). Therefore, emissivity varies with wavelength and is a property of the material. Kirchhoff's law states that when thermal equilibrium is assumed spectral emissivity is equal to spectral absorptivity ($\varepsilon(\lambda,T) = \alpha(\lambda,T)$). It allows measuring spectral emissivity or absorptivity from a surface using a spectrometer as spectral absorptance $\alpha(\lambda) = 1 - R(\lambda)$, since transmittance can be safely assumed to be zero for a thick stack.

The cosmic background can be considered as a blackbody at 3 K and will act as a heat sink for any solar cell capable of radiating out heat in the IR. A very broad band emissivity in the 3–20 μm range with high transmissivity in the 0.1–1.4 μm range is desired from the coating for the best radiative cooling output from a solar cell (Fig. 1). It is unlike daytime radiative cooling for terrestrial applications where only a window of 8–13 μm is available for transmission through earth's atmosphere. Due to presence of higher solar insolation and absence of a medium for convection, the solar cells will be operating at higher temperatures in

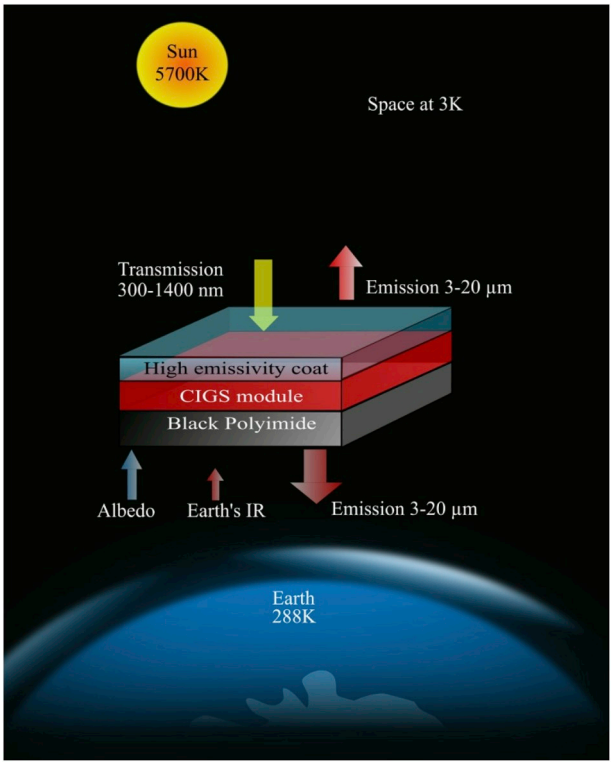

Fig. 1. Schematic of light and heat flow into the PV panel in orbit.

space than when on earth. Therefore, every stride towards achieving high emissivity space proof coating is of significance in making flexible solar cells for space applications a reality.

One of many ways to tune the thermal emission from a surface is to select a bulk material that has an optically active resonant peak in the required spectral region with high oscillator strengths [20]. Single compounds such as SiO_2, SiC, SiN, TiO_2 etc. lead to corresponding narrow emission peaks, whereas a combination of these results in multiple resonant narrow-band peaks. A coating derived from crosslinking of PSZ under low temperature is an example of such a material with characteristic multiple narrow-band peaks from various components of the polymeric chains [14]. The novelty of this approach is that it requires only a single deposition and processing step to achieve these multiple emission bands.

3. Experimental details

3.1. Synthesis and sample preparation

The organopolysilazane precursor, Durazane 1800 (Merck KGaA, Germany) was mixed with di-*n*-butyl ether (Fisher Scientific GmbH, Germany) solvent into a 50% w/w solution. The solution was stirred with a magnetic stirrer at room temperature for 1 h and then the solution was left standing for a minimum of 10 min before each dip. Dipping was carried out at room temperature with a dip coater built in-house using a stepper-motor fixed to a linear actuator and a motor-controller. A steel frame to support the flexible CIGS samples during dipping, draining and curing was designed. The samples were kept in an upright hanging position in all the phases until curing, using 0.5 mm small magnets placed on top of the frame as can be seen in Fig. 2a. The magnets keep the samples from bending. The small contact area of the magnets decreases the surface area lost by self-drip-off on the top surface during the coating and draining phase. With a larger steel frame, the same process was successfully scaled up for coating 14.6 cm × 14.6 cm modules. All samples had a dwell time of 10 s inside the solution before being hoisted. Curing was done in a convection oven (Binder GmbH, Germany) in air while samples were in a hanging position.

Both monolithically connected ultra-light CIGS samples on polyimide from Flisom AG, Switzerland and grid connected CIGS mini modules (5 cm × 1.2 cm) on polyimide from Ascent SOLAR, US were considered for the investigation (Fig. 2b and c). The Flisom samples were cut into 5 cm × 5 cm sizes from industry-made large modules (74.2 cm × 37.2 cm) for optical characterization. Whereas, the Ascent mini-modules due to their small size and exposed contacts, were used for electrical investigations. The front and back contact pads of Ascent modules were masked with Kapton band which was removed after curing.

3.2. Characterization

Optical characterization in the UV–Vis range was done with a UV–Vis–NIR (Cary 5000, Agilent, US) spectrometer. Microscope glass slides (VWR, Belgium) and Flisom samples (5 cm × 5 cm) were coated with a 0.5 m/min hoisting speed and cured at 180 °C for 1 h. For chemical and bond evolution analysis FTIR measurements (Spectrum 400, PerkinElmer, US) were done on coated polished wafers (PV-FZ wafer, Topsil, Denmark) in absorbance mode. Uncoated wafer was used as baseline. The wafer was dip coated with a hoisting speed of 0.5 m/min after which they were cured for 1 h at 180 °C.

Thickness and emissivity measurements were carried out with Flisom samples. The thickness of the coating was measured by cutting cross-sections using a FIB and observing them under the SEM (Neon 40 EsB, Zeiss, Germany). Sample preparation for SEM and FIB required cutting 5 cm × 5 cm into even smaller sizes and depositing a thin layer of conductive silver on top of the coating (for contrast). This makes the samples unusable for optical characterization process. Therefore, two sets of samples were created for correlation, each with same hoisting speed, one of which was used for SEM thickness and the other for emissivity measurement. All samples were cured under the same conditions for 1 h at 180 °C. Hemispherical spectral emissivity was calculated from (Equation (1)) reflection measurements in the wavelength range of 3–20 μm following the ECSS-Q-ST-70-09C standard [21] using a FTIR spectrometer (Vertex 80V, Bruker, Germany) with a gold integrating sphere. Hemispherical spectral reflectance measurements were done under vacuum and at room temperatures on coated and uncoated Flisom cut samples.

$$\varepsilon = \frac{\int_{3\mu m}^{20\mu m} \alpha_{sample}(\lambda).E_{blackbody}(\lambda)d\lambda}{\int_{3\mu m}^{20\mu m} E_{blackbody}(\lambda)d\lambda} \quad (1)$$

The Ascent samples used for electrical characterizations were pre-heated for 4 h at 180 °C before being coated, to make sure that the effect of the post-coated high temperature curing (at 180 °C for 1 h) had no influence on the electrical parameters and only the effect of the coating could be studied. IV and EQE were also measured every hour during the 4 h pre-heating step. No changes were observed after 2 h of pre-treatment heat step in either IV or EQE, indicating saturation. Nevertheless, we continued the heating step for 4 h. All IV measurements were done with AM1.5 spectra in accordance to standard test conditions.

4. Results and discussion

4.1. Coating thickness and cross-section

The thickness of the coating, deposited by dip coating process, can be varied by changing the hoisting speed and also by changing the concentration of the solution (other variables kept constant) as described by the Landau-Levich model [22]. The absorptivity or emissivity of the layer will vary with thickness of the PSZ layer. Therefore, we varied the hoisting speed of the substrate from the solution to experimentally determine the thickness of the PSZ coating on CIGS. For statistical significance, thicknesses of several points (more than 2) were measured from each FIB cross-section. Two FIB cuts were done per sample. An example of a FIB cut for a sample deposited with a 0.8 m/min hoisting speed is shown in Fig. 3a. The box plot shown in Fig. 3b includes all the thickness measurement points for each sample. As expected, the coating

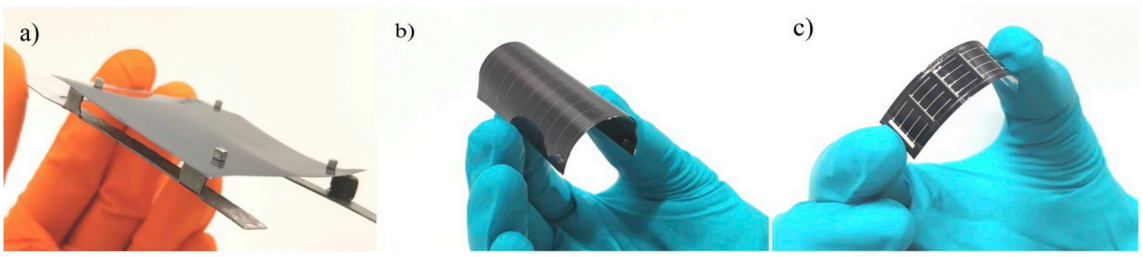

Fig. 2. a) Steel frame created to hold both Ascent and Flisom samples (shown here) in upright position, b) coated flexible Flisom 5 cm × 5 cm mini-module and c) coated 5 cm × 1.2 cm Ascent mini-module.

thickness increases with hoisting speed. The thickness of the coating can be varied from ~1.5 μm to ~3.5 μm just by varying the hoisting speed of the CIGS samples from a 50% w/w solution. It should be noted that the surface roughness of the top conductive layer (~500 nm) of the CIGS samples (as seen in Fig. 3a) mainly contributes to the standard deviation of the measurements.

4.2. Emissivity contribution

To study the influence of varying thickness of PSZ coating on total emissivity, reflection measurements in the spectra range of 3–20 μm for coated CIGS samples were measured. Total hemispherical emissivity was then calculated from the spectral reflectance measurements using Equation (1). The results are plotted in Fig. 4. As a general trend, we see that the total emissivity of the coating increases with coating thickness. It saturates after reaching a maximum of 0.72, even though samples prepared with 0.8 m/min or higher hoisting speed resulted in thicker coating. This result raises the possibility that the highest achievable emissivity of such a purely industry-based polymer precursor with no special post-processing step is reached with a thickness of ~3.2 μm. The inset graph shows the change of total emissivity with varying hoisting speed. The dotted lines are a guide to the eye. The results indicate that a coating of $\varepsilon = 0.7$ can be easily achieved with coating thickness greater than 2.7 μm obtained by hoisting speeds above 0.4 m/min with a 50% w/w solution. Having established how to achieve high emissivity coating, it was necessary to understand what contributes to the higher emissivity.

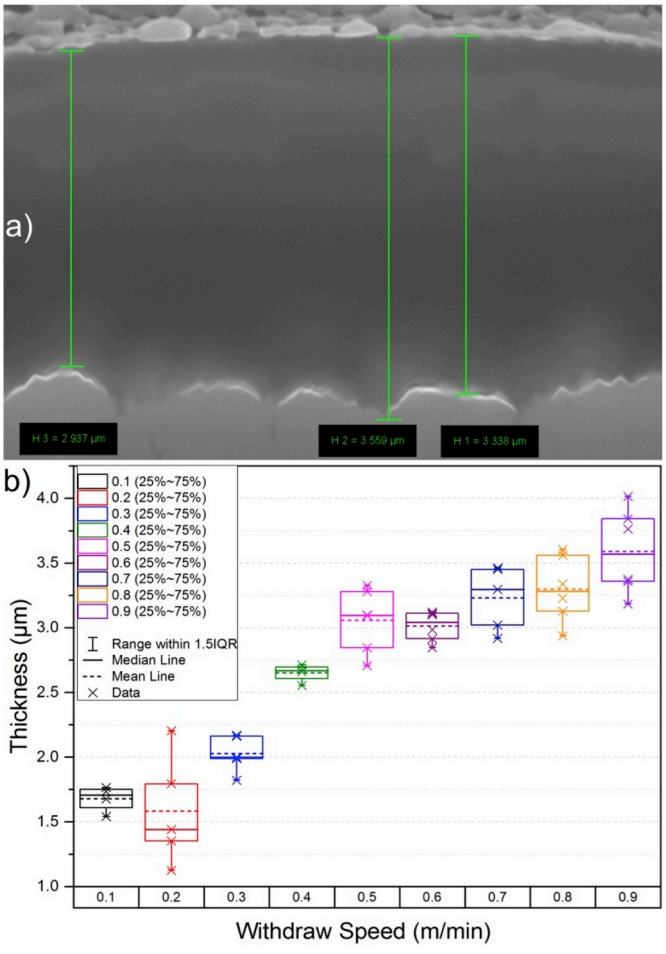

Fig. 3. a) SEM cross-section of top PSZ coating on CIGS cell done at 0.8 m/min withdraw speed. b) Variation of thickness of coating with hoisting speed on CIGS samples.

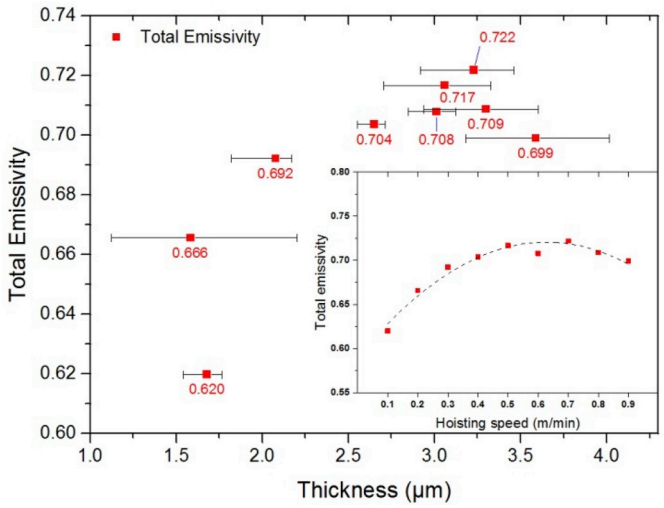

Fig. 4. Change of total emissivity with mean thickness of PSZ coat on CIGS substrates from 50% w/w solution during dip coating. Inset: variation of total emissivity with hoisting speed. The dashed line in the figure is a guide to the eye.

FTIR analysis is widely used to identify polymeric bonds in a material and several researchers reported and explained various curing dynamics of PDCs using FTIR analysis [13,23–31]. We analyzed FTIR spectra of the coating (on silicon wafers) together with the total hemispherical spectral emissivity measurements (on CIGS samples) to help us understand the reason behind the increase in emissivity seen with the PSZ coating. The comparison is shown in Fig. 5. The wavelength range of 3 μm–20 μm is considered for emissivity investigations (according to the ECSS standard). The FTIR measurements from 3333 cm^{-1} to 500 cm^{-1} matches that standard and enable us to understand the chemical bonding and the interaction of light with the bonds.

With curing temperatures below 300 °C, only crosslinking and shaping reactions are reached with the PSZ coating, leading to an incomplete ceramic phase conversion of SiO_X [31]. We observed similar FTIR absorbance peaks as in literature at ~3380 cm^{-1} (N–H stretching mode) overlapped with ~3320 cm^{-1} (O–H stretch), ~2164 cm^{-1} (Si–H symmetric stretching) and ~2968 cm^{-1} (C–H symmetric stretching) which are also known to be a reactive species [27,28]. As expected, the presence of these bands after 1 h of annealing indicates incomplete hydrolysis of the bonds with our curing process, as complete hydrolysis is only achieved at higher temperatures (~800 °C) [31]. The peak at ~1270 cm^{-1} (Si–CH_3 bending vibration mode) is an inactive species which is known not to take part in the curing kinetics. The broad band absorbance peak system seen in the range of 1270-970 cm^{-1} has a distinctive peak at 1036 cm^{-1} with a peak at the shoulder ~1100 cm^{-1}. It is representative of the Si–O–Si vibrational mode from the ladder like network of silsesquioxane [27,30]. Peaks seen at ~910 cm^{-1} and ~780 cm^{-1} can be assigned to Si–N stretching mode of Si–N–Si and Si–C of the same network [27].

All emissivity peaks (seen in Fig. 5b) are an outcome of the above said bond structures seen with FTIR. The largest contribution originates from the 3 peaks systems observed between 8 and 14 μm with individual emissivity peaks reaching >0.93. The Si–O–Si, Si–N–Si and Si–C chains are responsible for these peaks [14] and account for 56% of the emissive power in the complete wavelength range. With an increase in coating thickness or hoisting speed we observed an overall gain as well as noticeable gradual increase in between 14 and 20 μm where no peaks are present. This means with increasing thickness more polymeric chain molecules are available on the coating which results in an increase in overall absorption or emission intensity. We noticed that for a thicker coating (coated with >0.4 m/min) a peak at ~8.5 μm appears whereas for the thinner layers this peak (present in the shoulder) is not

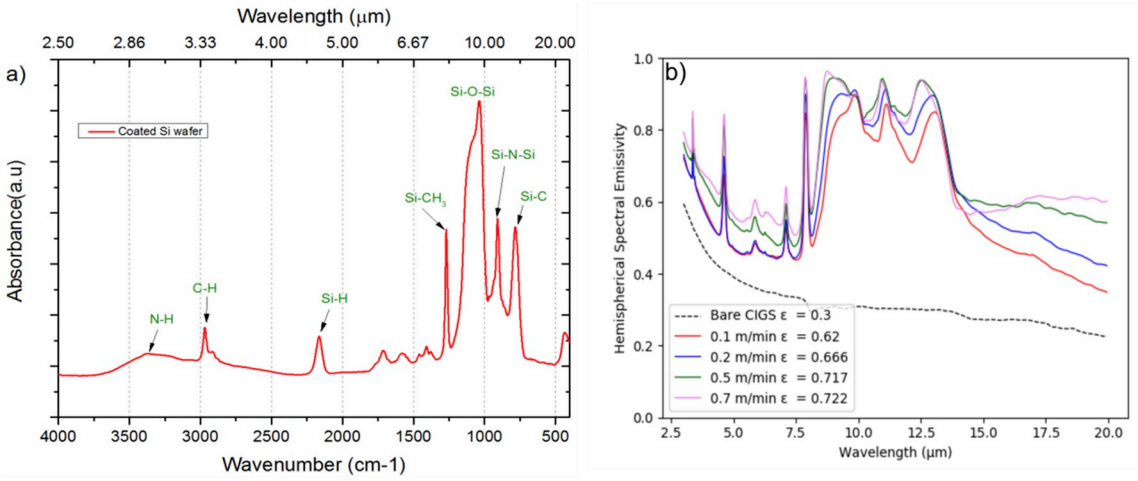

Fig. 5. a) FTIR absorbance spectra of polysilazane coating on polished silicon wafer b) Hemispherical spectral emissivity comparison on uncoated and coated CIGS samples. All samples underwent curing of 1 h at 180 °C. (For interpretation of the references to colour in this figure legend, the reader is referred to the Web version of this article.)

prominent. The peak at ~13 μm (Si–C stretching of Si–CH_3) can also be seen shifting to lower wavelength with an increase in thickness. Since the CH_3 group in the organopolysilazane derived polymeric chain remains inactive during curing, the shift could be attributed to the N in the chain being replaced by O, altering the mass and bond length of the group. Therefore, we see that more excitation energy is required to achieve the resonance frequency for this group with thicker coating.

A complete transition of the polymer chain to a Si–O–Si system is not favorable for our purpose since this will only lead to a narrow band emission in the range of 8–10 μm. Complete transition of Si–N–Si system to Si–O–Si system only happens at higher temperature (pyrolysis above 800 °C) with substitution of nitrogen atoms from the chain with oxygen from air resulting in increase in the Si–O–Si peak intensity and decrease in the Si–N–Si peak [25,29,31]. CIGS on polyimide substrates cannot be exposed to such high temperatures without major damage.

4.3. Optical properties of coating

The demand to have high emissive properties from a coating on top of a solar cell in the infrared region must coincide with good transmission properties in the UV–Vis region. A reduction in transmission would allow less light to be absorbed by the underlying CIGS cell and thereby fewer photo-generated charge carriers would be produced. PSZ coated glass and CIGS samples were used as substrates to do UV–Vis spectroscopy measurements as shown in Fig. 6. Both glass and CIGS samples were coated with a hoisting speed of 0.5 m/min and annealed at 180 °C for 1 h. No decrease in transmission and increase in reflection were observed over the entire wavelength range for the coated glass samples. The measurements from the coated samples follow that of the uncoated glass. This indicates that the refractive index of the coating is very similar to glass. For coated CIGS samples a significant drop in the reflection below 800 nm was observed. Anti-reflective properties of PSZ coatings have been reported before [14] and the decrease in reflection should be beneficial for the electrical performance of CIGS. The increase in reflection above 1400 nm (0.885 eV) should not interfere with solar cell performance as it is below the bandgap of CIGS (~1.1 eV). In general, the optical properties of the coating should have negligible influence on the solar cell performance.

4.4. Electrical characterization of coated CIGS module

Now that we demonstrated the optical properties and emissive properties of SiCNO coatings it is pertinent to study the effect of the coating and the process on the electrical performance of an active CIGS solar module. Separate CIGS mini modules were used for IV and EQE investigations. Both underwent the same pre-coating, coating and curing processes (described in Section 3.1 and 3.2). Both samples were coated with 0.5 m/min hoisting speed. IV measurements (seen in Fig. 7a) show no change in the I_{SC} and V_{OC} with the coating applied. The change in fill factor and efficiency after coating is very small and can be considered

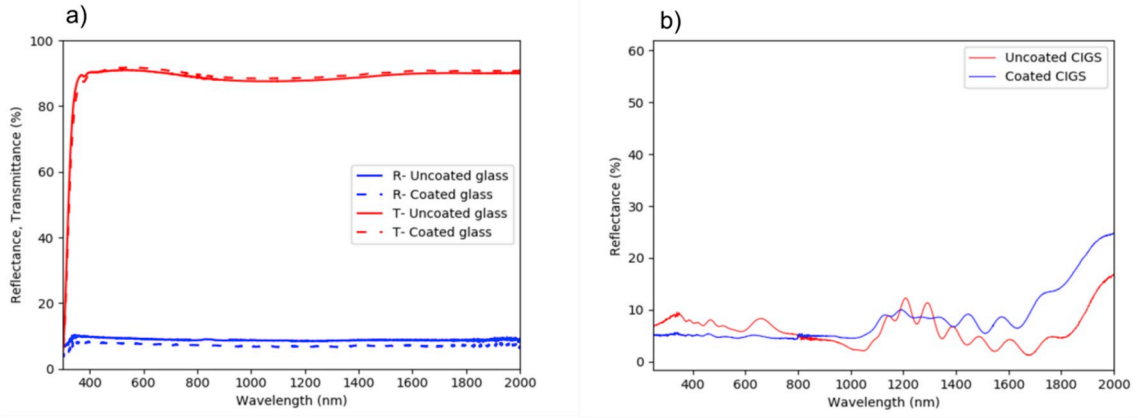

Fig. 6. a) Reflection and transmission measurements of coated and uncoated glass b) Reflection measurements from coated and uncoated CIGS samples.

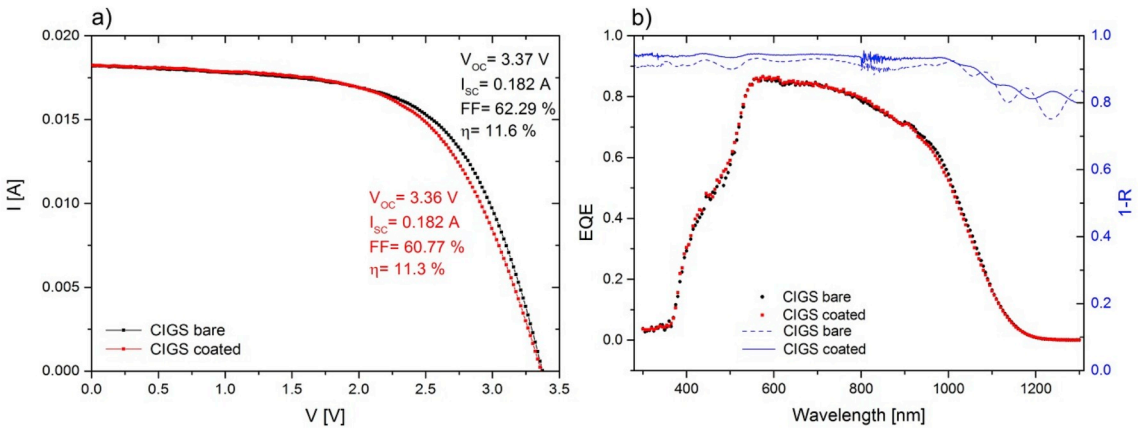

Fig. 7. a) IV characteristics CIGS solar module and b) external quantum efficiencies from a cell of the module before and after coating.

negligible. The resulting electrical parameters with our wet-coating process are very similar to previously published results of a double layer coat of SiO_2/Al_2O_3 using electron beam deposition by Shimazaki et al. [8]. No drop in the EQE (shown in Fig. 7b) was observed with the coating. However, absorption from the complete stack (300 nm–1000 nm) with coating increased but no significant increase in EQE was observed. The consistency of I_{SC} before and after coating (Fig. 7a) provides further verification. A similar decrease in reflection and increase in absorption was observed with the coated CIGS cells in Fig. 6b. Contrary to expectations, the lack of extra photo generated charge carriers means the light was absorbed within the top conductive layers before it could reach and be utilized in the absorber layer.

Overall, the electrical investigations revealed no detrimental effect of the PSZ based coating process on the solar cell functionality. The optical properties of the coating compliment the functioning of solar cell as we do not observe any optical losses in the SiCNO layer. Although the IV investigations were done under AM1.5, we believe the coating will have no adverse impact on the electrical behavior of the cells under AM0 since there was no change in the spectral response due to the coating.

4.5. Radiative cooling property

Due to the low electrical efficiency of CIGS, only ~10% of the absorbed AM0 spectra would be converted to electricity while the rest would be converted to heat. Since the only way to shed this excess heat from such thin film modules in space is radiative emission, an analysis is required to see what the integral emissive power gain from the coating is. A coated CIGS sample with hoisting speed of 0.5 m/min (see Fig. 6) with $\varepsilon = 0.717$ was considered for the analysis. Assuming the modules are at 100 °C in orbit, we can compare the thermal emittance capability of our coated sample to a non-coated one as shown in Fig. 8.

A theoretical black body at 100 °C can emit an integral spectral emittance of 290.47 W/m^2 within the range of 3–20 μm. With our coated system we can emit 203.65 W/m^2 in comparison to an uncoated one which can only emit 91.08 W/m^2. Since the resonance peaks of the coating align well with blackbody peak and it enables the stack to emit radiation with the highest intensity at orbit temperatures, an extra coating of only ~3 μm can enhance the emissive power of the solar cell by 123%. For terrestrial applications the window for emitting heat to space through earth's atmosphere lies in between 8 and 13 μm. The 3-peak system of Si–O–Si, Si–N–Si and Si–C contributes to a high $\varepsilon_{(8\text{–}13\ \mu m)} = 0.87$. It is more than two times the radiative emissive power through the window with a coating (83.5 W/m^2) in comparison to bare CIGS (29.58 W/m^2) at 70 °C. Therefore, SiCNO coatings are also highly beneficial for passive radiative cooling of terrestrial solar cells. Nevertheless, this analysis also implicitly indicates that a higher efficiency solar cell will lower the excess heat production to power generation

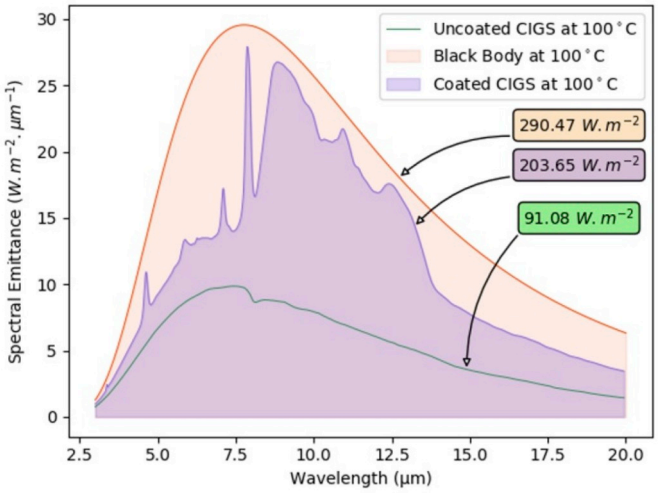

Fig. 8. Total integral emittance comparison of a blackbody, coated and uncoated module at 100 °C.

ratio. To better understand the benefit and temperature difference caused by such a coating on solar cells we simulated and studied in-orbit PV temperature profile in further details.

4.6. Orbital thermal analysis

The operational temperature of the solar cells in orbit is highly affected by the continuously changing environment due to their small heat capacity. To understand the influence of the LEO environment on the solar cells and the effect of different front emissivity, a thermal model was built where the PV cell temperature in the orbit was calculated using Thermal Desktop®. A circular LEO with an altitude of 650 km and a beta angle of 0° was assumed. As environmental heat fluxes, the incoming solar irradiation, Earth's albedo and IR fluxes were considered (See Table 1). The front side optical properties of the cell stack were taken into account based on the measurements of SiCNO coating on top of the CIGS cells. In this calculation, the front side absorptivity was set to be 0.93 based on measurement, and the emissivity was varied between 0.1 and 1.0, in order to evaluate the coating effect on the temperature. The rear side optical properties depend on the selection of the rear base material. The rear side material should have high emissivity to increase the heat rejection and low absorptivity to reduce the additional heating effect due to the albedo. The effect of high absorptivity of the rear side on the temperature is less significant than that of the emissivity. Additionally, the material should

Table 1
Value of parameters assumed for orbital thermal analysis.

Parameters	Values assumed
PV side epsilon	0.1–1.0
PV side alpha	0.93 (measured)
Back side epsilon	0.90
Back side alpha	0.90
Heat capacity	0
Electricity conversion	0%
Orbit	Altitude 650 km circular, $\beta = 0°$
Solar Constant	1354 W/m2
Albedo	0.35 (uniform)
Equivalent Earth temperature	250 K (uniform)

fulfill the necessary mechanical properties and environmental resistances and have low mass per unit area to be used behind the ultra-lightweight CIGS solar cells. Considering these points, we chose black polyimide as rear base material for this model and both emissivity and absorptivity were assumed to be 0.9. The realistic heat capacity of the PV stack is determined not only by the properties of PV cell itself but also by the base material, electrical instrumentations, and so on. For this calculation, the heat capacity was set to be zero, which would produce the hypothetical worst-case scenario and cause the most significant temperature variation. In addition, the reduction of heat load by the electricity generation of photovoltaic cells was not considered in this calculation.

Fig. 9 shows the resulting temperature profiles over one orbit with varying frontal emissivity. The steep rise and drop in temperature when coming out and going into eclipse were caused due to the zero heat capacity assumption. While the object is illuminated by the Sun, a front surface with higher emissivity shows lower temperature because of the larger heat rejection, which is preferred for the PV performance. By increasing the emissivity of the front surface from 0.3 to 0.7, the operating temperature would drop from 130 °C to 100 °C under illumination. Considering −0.47%/°C as the temperature co-efficient of maximum power for CIGS modules [32], the decrease of 30 °C due to the coating will result in 27% increase in maximum power output. Assuming a surface area of 20 m^2 of the GoSolAr membrane is available for PV installation, 62 min under illuminated orbit conditions and considering standard electrical parameters of Ascent 146 mm × 146 mm size modules [32], approximately 260 Wh of energy can be generated more per orbit for the payload. This could also mean fewer modules would be required to power a specified payload with the coating, thereby decreasing the overall system weight and cost. Additionally, during the eclipse phase, the high emissivity front surface absorbs larger amount of IR flux as it faces the Earth and hence, the PV does not cool down as much. This is also preferable, because the extreme low temperatures and stresses can be avoided. Therefore, the high emissivity on the photovoltaic front surface is beneficial for the in-orbit operation as the estimated energy savings with the coating has a sizeable impact on cost of launch due to decrease in overall system weight and size.

5. Conclusion

In summary, we demonstrated the exceptional optical characteristics of a single layer polymer derived high-ε coating on CIGS solar cells. We achieved $\varepsilon = 0.72$ with a ~3.2 μm layer of silicon oxycarbonitride coating cured under low temperatures. Electrical characterization of coated cells showed that the coating themselves, as well as the dip coating and post-processing steps had negligible effect on the electrical performance of the solar cells. The process can be scaled up easily and applied to other solar cell technologies to enhance emittance. The results are in good agreement to previously published literature. Our analysis suggests that with this coating the thermal radiative output of CIGS modules can be increased by a factor of 2.2. With emission peaks in between 8 and 13 μm, the coating is also very suitable for terrestrial PV

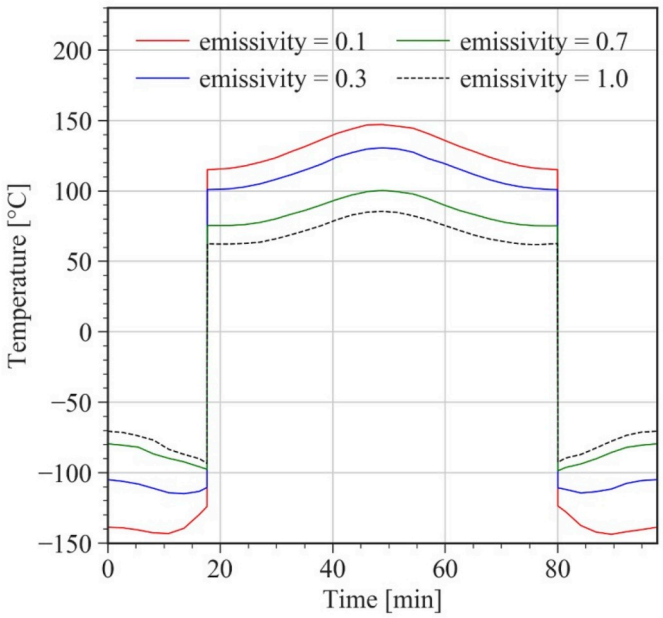

Fig. 9. Calculation of solar cell temperature at 650 km and 0° beta angle orbit with varying emissivity of the front surface.

module cooling. Using extreme case thermal analysis in LEO, we predict that our coating can decrease the temperature of the modules by 30 °C leading to ~27% increase in maximum power output in orbit at full irradiation situations. Moreover, due to the high front emissivity or absorptivity the modules will not be exposed to extreme cold conditions during eclipse. Despite the promising result, we believe that further decrease in module temperature can be achieved by blocking below band gap and high energy photons. With already proven flexibility and our results showing good thermal and electrical behavior, polysilazane derived coating is a good substitute for cover glasses used on solar cells for space applications.

Declaration of competing interest

None.

CRediT authorship contribution statement

Udayan Banik: Investigation, Methodology, Visualization, Writing - original draft. **Kaname Sasaki:** Investigation, Formal analysis, Writing - original draft. **Nies Reininghaus:** Conceptualization, Supervision, Writing - review & editing. **Kai Gehrke:** Validation, Writing - review & editing. **Martin Vehse:** Validation, Project administration, Supervision, Writing - review & editing. **Maciej Sznajder:** Investigation, Resources, Writing - review & editing. **Tom Sproewitz:** Writing - review & editing, Resources, Project administration, Funding acquisition. **Carsten Agert:** Supervision, Resources, Writing - review & editing, Funding acquisition.

Acknowledgement

We thank Oleg Sergeev for his help with SEM measurements, Jens Sürig Morieng for his help with building the dip coater. We also would like to thank Hosni Meddeb for his valuable suggestions and fruitful discussion while preparing the manuscript and Colleen Lattyak and Maximilian Götz for proofreading earlier versions of the manuscript. The authors thank DLR Space Research and Development and Energy branch for funding this activity.

Appendix A. Supplementary data

Supplementary data to this article can be found online at https://doi.org/10.1016/j.solmat.2020.110456.

Declaration of interests

The authors declare that they have no known competing financial interests or personal relationships that could have appeared to influence the work reported in this paper.

References

[1] R. Spores, J. Monheiser, B.P. Dempsey, D. Wade, K. Creel, D. Jacobson, G. Drummond, A solar electric propulsion cargo vehicle to support NASA lunar exploration program, 25th International Electric Propulsion Conference 31 (2005).

[2] K. Otte, L. Makhova, A. Braun, I. Konovalov, Flexible Cu(In,Ga)Se2 thin-film solar cells for space application, Thin Solid Films 511–512 (2006) 613–622, https://doi.org/10.1016/j.tsf.2005.11.068.

[3] S. Matsuda, M. Imaizumi, O. Anzawa, S. Kawakita, T. Sumita, K. Aoyama, N. Tanioka, Radiation effects in space on solar cells developed for terrestrial use demonstrated by MDS-1, 3rd World Conference on, Photovoltaic Energy Conversion 1 (2003) 642–645.

[4] S. Kawakita, M. Imaizumi, T. Sumita, K. Kushiya, T. Ohshima, M. Yamaguchi, S. Matsuda, S. Yoda, T. Kamiya, Super radiation tolerance of CIGS solar cells demonstrated in space by MDS-1 satellite, in: 3rd World Conference on Photovoltaic Energy Conversion, 2003, pp. 693–696.

[5] S. Kawakita, M. Imaizumi, M. Takahashi, Space Experiments of Cu (In Ga) Se 2 Thin-Film Solar Cells by Japanese Small Satellites, 26th European Photovoltaic Solar Energy Conference and Exhibition, 2011.

[6] K. Weinert, A. Jasenek, U. Rau, Consequence of 3-MeV electron irradiation on the photovoltaic output parameters of Cu(In,Ga)Se2 solar cells, Thin Solid Films 431–432 (2003) 453–456, https://doi.org/10.1016/S0040-6090(03)00181-0.

[7] S. Kawakita, M. Imaizumi, M. Yamaguchi, K. Kushiya, T. Ohshima, S. Matsuda, In-situ measurement of degradation of Cu(In,Ga)Se2 thin film solar cells during electron and proton irradiations, in: Twenty-Ninth IEEE Photovoltaic Specialists Conference, 2002, https://doi.org/10.1109/PVSC.2002.1190764.

[8] K. Shimazaki, M. Imaizumi, K. Kibe, SiO2 and Al2O3/SiO2 coatings for increasing emissivity of Cu(In, Ga)Se2 thin-film solar cells for space applications, Thin Solid Films 516 (2008) 2218–2224, https://doi.org/10.1016/j.tsf.2007.07.159.

[9] S.H. Liu, E.J. Simburger, J. Matsumoto, A. Garcia, J. Ross, J. Nocerino, Evaluation of thin-film solar cell temperature coefficients for space applications, Prog. Photovoltaics Res. Appl. 13 (2005) 149–156, https://doi.org/10.1002/pip.602.

[10] T. Sproewitz, J.T. Grundmann, F. Haack, M. Hillebrandt, H. Martens, S. Meyer, S. Reershemius, N. Reininghaus, K. Sasaki, P. Seefeldt, O. Sergeev, P. Spietz, M. Sznajder, N. Toth, M. Vehse, T. Wippermann, M.E. Zander, GoSolAr – a gossamer solar array concept for high power spacecraft applications using flexible photovoltaics, in: 2019 IEEE Aerospace Conference, 2019, pp. 1–14, https://doi.org/10.1109/AERO.2019.8741868.

[11] T. Sproewitz, U. Banik, J.-T. Grundmann, F. Haack, M. Hillebrandt, H. Martens, S. Meyer, S. Reershemius, N. Reininghaus, K. Sasaki, P. Seefeldt, O. Sergeev, P. Spietz, M. Sznajder, N. Toth, M. Vehse, T. Wippermann, M.E. Zander, Concept for a Gossamer solar power array using thin-film photovoltaics, CEAS Space Journal 12 (1) (2020) 125–135, https://doi.org/10.1007/s12567-019-00276-6.

[12] J.T. Grundmann, P. Spietz, P. Seefeldt, T. Spröwitz, GOSSAMER deployment systems for flexible photovoltaic, in: 67th International Astronautical Congress.

[13] M. Pscherer, M. Günthner, C.A. Kaufmann, A. Rahm, G. Motz, Thin-film silazane/alumina high emissivity double layer coatings for flexible Cu(In,Ga)Se 2 solar cells, Sol. Energy Mater. Sol. Cell. 132 (2015) 296–302, https://doi.org/10.1016/j.solmat.2014.09.015.

[14] M. Günthner, M. Pscherer, C. Kaufmann, G. Motz, High emissivity coatings based on polysilazanes for flexible Cu(In,Ga)Se2 thin-film solar cells, Sol. Energy Mater. Sol. Cell. 123 (2014) 97–103, https://doi.org/10.1016/j.solmat.2014.01.027.

[15] L. Hu, M. Li, C. Xu, Y. Luo, Y. Zhou, A polysilazane coating protecting polyimide from atomic oxygen and vacuum ultraviolet radiation erosion, Surf. Coating. Technol. 203 (2009) 3338–3343, https://doi.org/10.1016/j.surfcoat.2009.04.019.

[16] L. Hu, M. Li, C. Xu, Y. Luo, Perhydropolysilazane derived silica coating protecting Kapton from atomic oxygen attack, Thin Solid Films 520 (2011) 1063–1068, https://doi.org/10.1016/j.tsf.2011.10.011.

[17] W. Li, Y. Shi, K. Chen, L. Zhu, S. Fan, A comprehensive photonic approach for solar cell cooling, ACS Photonics 4 (2017) 774–782, https://doi.org/10.1021/acsphotonics.7b00089.

[18] M.A. Kecebas, M.P. Menguc, A. Kosar, K. Sendur, Passive radiative cooling design with broadband optical thin-film filters, J. Quant. Spectrosc. Radiat. Transf. 198 (2017) 179–186, https://doi.org/10.1016/j.jqsrt.2017.03.046.

[19] M.M. Hossain, M. Gu, Radiative cooling: principles, progress, and potentials, Adv. Sci. 3 (2016) 1500360, https://doi.org/10.1002/advs.201500360.

[20] D.G. Baranov, Y. Xiao, I.A. Nechepurenko, A. Krasnok, A. Alù, M.A. Kats, Nanophotonic engineering of far-field thermal emitters, Nat. Mater. 18 (9) (2019) 920–930, https://doi.org/10.1038/s41563-019-0363-y.

[21] ECSS Executive Secretariat, ECSS-Q-ST-70-09C: Space Product Assurance-Measurements of Thermo-Optical Properties of Thermal Control Materials, 2008.

[22] B. Levich, L. Landau, Dragging of a liquid by a moving plate, Acta Physicochim. URSS 17 (1942).

[23] G. Barroso, Q. Li, R.K. Bordia, G. Motz, Polymeric and ceramic silicon-based coatings-a review, J. Mater. Chem. 7 (2019) 1936–1963, https://doi.org/10.1039/c8ta09054h.

[24] J.-S. Lee, J.-H. Oh, S.-W. Moon, W.-S. Sul, S.-D. Kim, A technique for converting perhydropolysilazane to SiOx at low temperature, Electrochem. Solid State Lett. 13 (2009), https://doi.org/10.1149/1.3264092.

[25] K. Wang, M. Günthner, G. Motz, B.D. Flinn, R.K. Bordia, Control of surface energy of silicon oxynitride films, Langmuir 29 (2013) 2889–2896, https://doi.org/10.1021/la304307y.

[26] Frank Bauer, Ulrich Decker, Andreas Dierdorf, Horst Ernst, Preparation of moisture curable polysilazane coatings: Part I. Elucidation of low temperature curing kinetics by FT-IR spectroscopy, Prog. Org. Coating 53 (2005), https://doi.org/10.1016/j.porgcoat.2005.02.006.

[27] S. Rossi, F. Deflorian, M. Fedel, Polysilazane-based coatings: corrosion protection and anti-graffiti properties, Surf. Eng. 35 (2019) 343–350, https://doi.org/10.1080/02670844.2018.1465748.

[28] P. Furtat, M. Lenz-Leite, E. Ionescu, R.A.F. Machado, G. Motz, Synthesis of fluorine-modified polysilazanes via Si–H bond activation and their application as protective hydrophobic coatings, J. Mater. Chem. A 5 (2017) 25509–25521, https://doi.org/10.1039/C7TA07687H.

[29] T. Ohishi, S. Sone, K. Yanagida, Preparation and gas barrier characteristics of polysilazane-derived silica thin films using ultraviolet irradiation, MSA 5 (2014) 105–111, https://doi.org/10.4236/msa.2014.53015.

[30] M. Fedel, E. Callone, S. Diré, F. Deflorian, M.-G. Olivier, M. Poelman, Effect of Na-Montmorillonite sonication on the protective properties of hybrid silica coatings, Electrochim. Acta 124 (2014) 90–99, https://doi.org/10.1016/J.ELECTACTA.2013.11.006.

[31] P. Colombo, G. Mera, R. Riedel, G.D. Sorarù, Polymer-derived ceramics: 40 Years of Research and innovation in advanced ceramics, J. Am. Ceram. Soc. 73 (2010), https://doi.org/10.1111/j.1551-2916.2010.03876.x no-no.

[32] Ascent SOLAR, Bare Modules Mid-Scale Group. http://www.ascentsolar.com/bare-modules.html. (Accessed 17 September 2019).